Percolation via Combined Electrostatic and Chemical Doping in Complex Oxide Films

Peter P. Orth,[1] Rafael M. Fernandes,[1] Jeff Walter,[2] C. Leighton,[2] and B. I. Shklovskii[1,3]
[1]School of Physics and Astronomy, University of Minnesota, Minneapolis, Minnesota 55455, USA
[2]Department of Chemical Engineering and Materials Science, University of Minnesota, Minneapolis, Minnesota 55455, USA
[3]Fine Theoretical Physics Institute, University of Minnesota, Minneapolis, Minnesota 55455, USA
(Received 18 May 2016; published 7 March 2017)

Stimulated by experimental advances in electrolyte gating methods, we investigate theoretically percolation in thin films of inhomogeneous complex oxides, such as $La_{1-x}Sr_xCoO_3$ (LSCO), induced by a combination of bulk chemical and surface electrostatic doping. Using numerical and analytical methods, we identify two mechanisms that describe how bulk dopants reduce the amount of electrostatic surface charge required to reach percolation: (i) bulk-assisted surface percolation and (ii) surface-assisted bulk percolation. We show that the critical surface charge strongly depends on the film thickness when the film is close to the chemical percolation threshold. In particular, thin films can be driven across the percolation transition by modest surface charge densities. If percolation is associated with the onset of ferromagnetism, as in LSCO, we further demonstrate that the presence of critical magnetic clusters extending from the film surface into the bulk results in considerable enhancement of the saturation magnetization, with pronounced experimental consequences. These results should significantly guide experimental work seeking to verify gate-induced percolation transitions in such materials.

DOI: 10.1103/PhysRevLett.118.106801

Introduction.—The rapidly growing field of complex oxide heterostructures provides many opportunities for the observation of new physical phenomena, with promising applications in future electronic devices [1–3]. Examples include strain engineering to control structural and electronic ground states [1–4], realization of novel two-dimensional electron gases at oxide interfaces [3,5,6], and the observation of interfacial magnetic [1–3,7] and superconducting states [1–3]. Because of the lower charge carrier densities in these materials ($n \simeq 10^{21}$ cm^{-3}) compared to conventional metals ($n \simeq 10^{23}$ cm^{-3}), surface electrostatic or electrochemical control of these novel properties via the electric field effect also becomes an exciting possibility [2,8–10].

Stimulated by the above situation, high-κ dielectrics, ferroelectric, and electrolyte gating have been successfully employed to electrostatically induce and control large charge densities in these materials [2,8–10]. Particularly prominent recent progress has been made with ionic liquid and gel gating, the surface carrier densities achieved routinely exceeding $s \simeq 10^{14}$ cm^{-2}, corresponding to modulation of significant fractions of an electron (or hole) per unit cell [2,8–10]. This has, for example, enabled reversible external electrical control of oxide electronic phase transitions from insulating to metallic [11–14], to a superconducting state [15–17], or from paramagnetic to magnetically ordered phases [18,19]. Nevertheless, attainment of sufficient charge density to induce the phase transitions of interest remains a challenge in many cases, due to the need for $s \simeq 10^{15}$ cm^{-2}. In such cases one obvious strategy is to employ a combination of chemical and electrostatic doping, bringing the material close to some electronic and/or magnetic phase boundary by chemical substitution, then using surface electrostatic tuning of the carrier density to reversibly traverse the critical point.

The work presented here focuses on such combined electrostatic surface and bulk chemical doping and

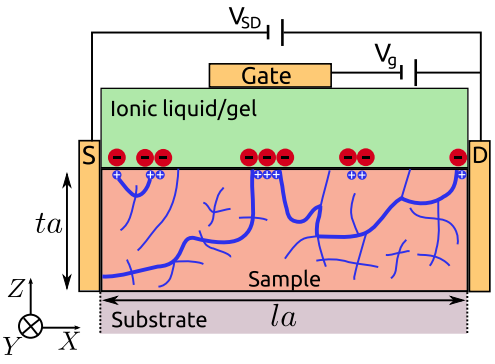

FIG. 1. Schematic setup showing a thin-film sample (red) of thickness ta and area $la \times la$, where a is the lattice constant, with large finite clusters (blue) due to bulk doping. The ionic liquid or gel (light green) on top of the sample induces a number of holes (blue spheres) at the top surface—proportional to the applied gate voltage V_g. Red spheres denote anions in the ionic liquid or gel that move towards the surface due to the applied voltage. For bulk doping close to percolation $x_c - x \ll 1$ (surface-assisted bulk percolation), electrostatically induced holes connect finite bulk clusters at the surface resulting in a conducting path (highlighted) between source (S) and drain (D) electrodes. The highlighted upper left-hand cluster shows bulk bridges connecting two surface clusters, which is the dominant effect of bulk dopants for $x \ll x_c$ (bulk-assisted surface percolation).

resulting electronic and/or magnetic percolation transitions. This is an important situation in complex oxide materials due to the widespread observation of electronic and magnetic inhomogeneity (as in manganites [20], cuprates [21], and cobaltites [22,23], for example), where many transitions, such as from insulator to metal or from short- to long-range magnetism, are percolative in nature. We approach this problem using classical percolation theory [24,25]. While our analysis and results are general, and could apply to percolation transitions in various materials, in this Letter we are motivated by physics of the perovskite oxide cobaltite, $La_{1-x}Sr_xCoO_3$ (LSCO), which undergoes a percolation transition from insulator to metal at $x_{c,\mathrm{LSCO}} \simeq 0.18$ [22,23,26].

In the parent compound $LaCoO_3$ ($x = 0$), the Co^{3+} ($3d^6$) ions adopt the $S = 0$ spin state as $T \to 0$, and the material is a diamagnetic semiconductor. Substituting Sr^{2+} for La^{3+} induces holes, changing the formal valence state of a neighboring Co ion to 4+, which is in a $S > 0$ spin state. The subsequent evolution from insulator to metal (due to hole transfer between nearest-neighbor Co^{4+}) and short- to long-range ferromagnetic correlations is caused by percolation of nanoscopic ferromagnetic hole-rich clusters [22,23,26]. Very thin (few unit cell thick) films of LSCO are the natural target for field-effect gating experiments, as significant modulation of the charge carrier density is confined to a narrow layer close to the surface. The layer width is of the order of the electrostatic screening length, which is typically one or two unit cells [2,8–10] due to the large carrier densities ($n \simeq 10^{21}$ cm^{-3}) in significantly doped LSCO.

The theoretical study of percolation phenomena in correlated systems has a long history [24,25,27–31]. The combination of bulk chemical and surface electrostatic doping, however, defines an unusual percolation problem that is thus far largely unexplored theoretically. The schematic setup is shown in Fig. 1, where the total (top) surface carrier density is given by

$$s = x + \Delta s. \tag{1}$$

It arises from doping by both chemical substitution of a fraction of lattice sites x and electrostatic gating of a fraction of surface lattice sites Δs, and implies $s \leq 1$.

In this work we identify two different percolation phenomena: bulk-assisted surface percolation and surface-assisted bulk percolation, which are schematically depicted in Fig. 1. The first case applies to a system that is initially far away from the (thickness-dependent) bulk percolation threshold $x_c(t)$. In addition to the trivial effect that bulk doping ($x > 0$) increases s according to Eq. (1), percolation on the surface is further facilitated by diluted bulk dopants providing bridges that connect disjunct finite surface clusters. In the second case, where the bulk chemical doping level is close to the percolation threshold, $x_c(t) - x \ll 1$, we find that small Δs helps to reach bulk percolation by connecting large finite bulk clusters on the surface. We show that the amount of surface charge Δs_c that must be induced electrostatically to reach percolation grows moderately with $(x_c - x)$ for thin films, but increases sharply for thicker films.

Numerical modeling of percolation.—To derive our results, we consider the site percolation problem on the cubic lattice of size $la \times la \times ta$ along the X, Y, and Z axes defined in Fig. 1, where a is the lattice constant and l, t are integers ($t \leq l$). This geometry describes films of thickness ta and surface area $(la)^2$. We note that the new scaling laws in Eqs. (2), (3), (4), and (6) that we derive below are *universal* and therefore independent of microscopic details such as lattice symmetry or local connectivity. They thus apply to LSCO and other experimental systems even though the percolation thresholds, which are *not* universal quantities, may differ from that of a cubic lattice $x_c^{3\mathrm{D}} = 0.31$ [32]. The thin-film percolation problem is solved using the numerical algorithm described in Refs. [33,34]. Starting from an empty lattice, a fraction x of sites is first randomly filled in the whole lattice to simulate bulk chemical doping. We verify that the bulk doping percolation threshold on the isotropic cubic lattice ($l = t$) lies at $x_c^{3\mathrm{D}} = 0.31$, and increases for $t < l$; i.e., $x_c(t) > x_c(l) \equiv x_c^{3\mathrm{D}}$ [24]. To study the role of surface doping, we stop at a bulk doping level $x < x_c(t)$ and subsequently add a fraction Δs of sites exclusively on the top surface layer to simulate electrostatic gating. The total surface density of sites at the top surface is then given by Eq. (1). While electrostatically doping the system, we continuously monitor whether a percolating path exists between the two side surfaces at $X = 0$ and $X = la$. We define the critical total density of sites at the top surface that is required for percolation between the side surfaces as s_c. The amount of charge density that must be transferred via electrostatic doping is then denoted Δs_c.

In Fig. 2(a), we show numerical results for Δs_c as a function of the starting bulk chemical doping level x. Figure 2(b) shows s_c as a function of x. For pure surface doping, $x = 0$, we find the percolation threshold of the 2D square lattice, $\Delta s_c(0) = 0.59$ [25]. For small $x \ll x_c(t)$, the behavior of $\Delta s_c(x)$ depends only weakly on the film thickness t. In contrast, for $x_c(t) - x \ll 1$ the function $\Delta s_c(x)$ depends strongly on the thickness t, displaying a sharp enhancement as x decreases for thick films but a much more gradual one for thin films.

Analytical theory.—To develop an analytical scaling theory [24], we focus on three limits: (i) $x \ll x_c(t)$, (ii) $x_c^{3\mathrm{D}} - x \ll 1$, and (iii) $x_c(t) - x \ll 1$, which are indicated by yellow rectangles in Fig. 2(a). The first case can be described as bulk-assisted surface percolation and the other two by surface-assisted bulk percolation.

(i) For $x \ll x_c(t)$, we have $s_c(0) - s_c(x) \ll 1$: the system is close to the 2D percolation threshold on the

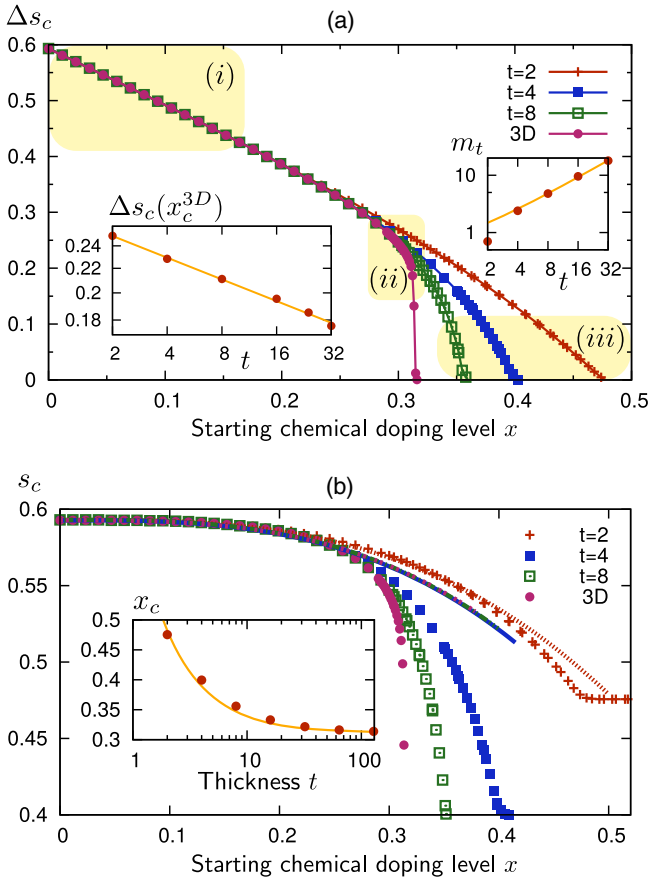

FIG. 2. (a) Surface charge density Δs_c that must be electrostatically induced to reach percolation, as a function of starting bulk chemical doping level x. Different curves correspond to different thicknesses t and are obtained from extrapolating results for system sizes $l \times l \times t$ with $l = 32, 64, 128$ to $l^{-1} \to 0$ and are averaged over at least 4.1×10^5 disorder realizations. The curve labeled "3D" is for $t = l$. The left inset shows that Δs_c at the bulk percolation threshold $x_c^{3D} = 0.31$ obeys Eq. (4) (yellow line) with $c_2 = 0.27$ and $\nu_{\text{fit}} = 0.89 \pm 0.01$. The right inset shows the slope of $s_c - x_c = m_t(x_c - x)$ close to $x_c(t) - x \ll 1$, verifying Eq. (6), with $c_5 = 0.56$. Yellow rectangles mark the three regimes labeled (i)– (iii), addressed by our analytical theory. (b) Total surface charge at percolation s_c as a function of x. The lines are fits of the numerical results according to Eq. (2) with $b = 0.91$ for $t = 2$ and $b = 1.12$ for $t = 4$, 8, l. The inset shows the thickness-dependent bulk percolation threshold $x_c(t)$ for purely chemical doping. The yellow line obeys Eq. (5) with $x_c^{3D} = 0.312$, $\nu = 0.88$ [32], and $c_3 = 1.21$.

surface, but far from percolation in the bulk. As a result, the typical size of bulk clusters is rather small. These small bulk clusters (away from the surface) can still assist percolation at the surface by providing short bridges across missing links between disconnected finite large surface clusters, as shown in Fig. 1. Since the smallest possible bulk bridge consists of three sites below the surface, at $x \ll 1$ the main contribution of the bulk doping arises from such bridges, yielding

$$s_c(x) = s_c(0) - bx^3. \tag{2}$$

As shown in Fig. 2(b), this equation, with weakly t-dependent coefficient b, describes the numerical results well for $s_c(0) - s_c(x) \ll 1$; for $t = 2$ it is even applicable over almost the full range of doping levels up to x_c.

(ii) In the regime of small $x_c^{3D} - x \ll 1$, the 3D bulk is close to the percolation threshold, but the surface concentration is far from the surface percolation threshold. Thus, while large critical finite clusters exist in the bulk, with a typical size of $\xi(x) \sim a(x_c^{3D} - x)^{-\nu}$ and correlation length exponent $\nu = 0.88$ [25,32], the largest surface clusters remain small.

Let us first discuss the case of an infinite isotropic 3D system. If sites were randomly added in the bulk, an infinite cluster connecting $X = 0$ and $X = la$, which looks like a network of links and nodes with typical separation $\xi(x)$, would occur after adding $N = N_0(x_c^{3D} - x)l^3$ sites, with $N_0 \simeq 2$. Because this infinite cluster provides percolation inside a layer of height $\xi(x)$ below the surface, the number of sites $\Delta N = N_0(x_c^{3D} - x)l^2\xi(x)/a$ we have added to this layer is sufficient to induce percolation along the layer. We assume that addition of sites to any of the ξ/a planes parallel to the surface within this layer equally contributes to the probability to connect critical clusters. Then, instead of homogeneously doping the layer of volume $(la)^2\xi(x)$, we can reach percolation by adding all these sites to the surface plane only. This yields a critical surface density of

$$s_c(x) = x_c^{3D} + \frac{\Delta N}{l^2} = x_c^{3D} + c_1(x_c^{3D} - x)^{1-\nu}, \tag{3}$$

with a nonuniversal constant c_1. We see that since $\nu < 1$, connecting bulk clusters on the surface can be done by very small surface addition Δs at $x_c^{3D} - x \ll 1$. Scaling in Eq. (3) only holds for $(x_c^{3D} - x)^{1-\nu} \ll 1$. Since $1 - \nu = 0.12 \ll 1$ [25,32], the validity of Eq. (3) is thus limited to a tiny region of x close to x_c^{3D}, which explains the sharp rise of $\Delta s_c(x)$ for $t = l$ (3D) in Fig. 2.

A finite thickness t of the film introduces another length scale, which cuts off the scaling behavior of Eq. (3) as soon as $\xi(x) > ta$, and Eq. (3) is replaced by

$$s_c(x) = x_c^{3D} + c_2 t^{1-1/\nu}, \tag{4}$$

with nonuniversal constant c_2. We numerically verify this scaling behavior at $x = x_c^{3D}$, as shown in the (left) inset of Fig. 2(a). A fit to our data yields $\nu_{\text{fit}} = 0.89 \pm 0.01$, confirming the expected scaling with $\nu = 0.88$ [25,32]. To derive Eq. (4), we first notice that the bulk percolation threshold $x_c(t)$ of a film of thickness t is reached when an infinite bulk cluster with correlation length $\xi[x_c(t)] \leq ta$ appears. From this, it follows that [24]

$$x_c(t) = x_c^{3D} + c_3 t^{-1/\nu}, \tag{5}$$

with nonuniversal constant $c_3 = 1.21$, which is in agreement with our numerical results shown in the inset of Fig. 2(b). Therefore, to achieve percolation at $x \simeq x_c^{3D}$, a film with width t must acquire $\Delta N = c_4[x_c(t) - x_c^{3D}]tl^2 = c_2 l^2 t^{1-1/\nu}$ filled sites, where c_4 is a nonuniversal constant. As above, we assume that we can reach the percolation threshold by bringing all these sites into the surface plane by electrostatic gating, yielding Eq. (4). Note that Eq. (4) crosses over to Eq. (3) at $\xi(x) = ta$.

(iii) We now investigate s_c for $x_c(t) - x \ll 1$. In this regime, it holds that $\xi(x) > ta$, since the correlation length at $x_c(t)$ fulfills $\xi[x_c(t)] = ta$. We find that $\Delta N = [x_c(t) - x]l^2 t$ sites should be added to the system in order to reach percolation, such that the critical surface percolation threshold obeys

$$s_c(x) = x_c(t) + c_5 t[x_c(t) - x], \tag{6}$$

with nonuniversal constant c_5. We demonstrate in the (right) inset of Fig. 2(a) that our numerical results follow this scaling relation of the slope $m_t = c_5 t$, with $c_5 = 0.56$. Note that the scaling breaks down for the thinnest system, $t = 2$, which is instead described by Eq. (2) over the full range of bulk doping levels x [see Fig. 2(b)].

The key insight from our results is that bulk chemical doping largely reduces the amount of electrostatic surface charge Δs_c required to reach percolation (compared to the 2D value) in a region of initial chemical doping levels $x_c^{3D} < x < x_c(t)$. In this regime, the critical surface charge s_c scales with the thickness according to Eq. (6) and therefore grows quickly for thicker films. The underlying physical phenomenon is that less surface charge must be transferred by electrostatic gating if percolation is induced by connecting finite large bulk clusters on the surface rather than creating a percolating path that is confined to the surface alone. The width of this region $x_c - x_c^{3D} \propto t^{-1/\nu}$ rapidly narrows for thicker films. For smaller x, the dominant effect of the bulk dopants is to act as short bridges between disconnected surface clusters. This reduces the number of surface sites that must be filled to reach percolation only slightly compared to the 2D case [see Eq. (2)].

Enhanced surface magnetization.—If the percolation transition is associated with ferromagnetic ordering, as for LSCO, the extension of the percolating cluster from the surface into the bulk leads to a dramatic volume enhancement of the surface saturation magnetization M_s in the case of surface-assisted bulk percolation [cases (ii) and (iii)]. To capture this equilibrium phenomenon, in Fig. 3 we show the size (i.e., number of sites) of the largest cluster N_c (per surface area l^2) as a function of electrostatic doping Δs. Beyond the percolation threshold $\Delta s > \Delta s_c(x)$, this cluster percolates and its size, i.e., number of sites with ferromagnetically polarized Co spins, is proportional to the surface saturation magnetization $M_s \propto N_c/l^2$. For small

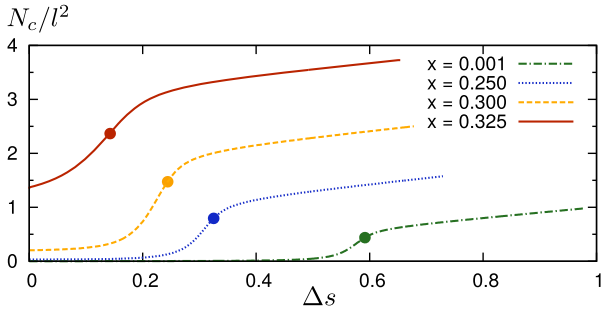

FIG. 3. Surface density of the largest cluster in the system N_c/l^2 as a function of electrostatic doping Δs in a film of thickness $t = 16$. Dots indicate percolation thresholds $\Delta s_c(x)$. For $\Delta s > \Delta s_c$, N_c/l^2 is proportional to the surface saturation magnetization M_s. The plot shows the large enhancement of M_s due to the extension of the infinite cluster deep into the bulk.

doping levels, we observe regular surface percolation at $\Delta s_c \simeq 0.59$. The percolated path is almost entirely confined to the top surface layer and the magnetization enhancement is absent: $N_c/l^2 \lesssim 1$. However, if the system is initially doped closer to the (bulk) percolation threshold x_c, the percolating cluster extends significantly into the bulk and we observe $N_c/l^2 > 1$. As the (fractal) dimension of this cluster exceeds $d = 2$, we find that N_c/l^2 becomes as large as 4 for a film of thickness $t = 16$ (a fully magnetized film corresponds to $N_c/l^2 = t$). This shows that bulk doping ultimately generates a much larger saturation magnetization, because of the inclusion of preformed clusters of spin polarized sites. We further predict an unusual depth profile of magnetization $M_s(z)$ as a function of distance z from the surface, which can be directly experimentally measured using polarized neutron reflectometry or indirectly inferred using x-ray magnetic circular dichroism (XMCD) or the magneto-optical Kerr effect (MOKE).

Conclusions.—Motivated by existing and ongoing experiments on complex oxide thin films, we have studied a new percolation problem, where bulk chemical doping is combined with electrostatic doping of the surface. We have derived new analytical formulas describing universal scaling behavior of the electrostatic percolation threshold and explored the full crossover from bulk to surface percolation numerically. Experimental predictions that follow from our analysis are the following. (i) The critical surface charge density at percolation s_c depends only weakly on the starting bulk doping level x, except in proximity to the bulk percolation transition $x_c^{3D} < x < x_c(t)$. The crossover from surface-assisted to bulk-assisted percolation occurs more abruptly for thicker films. Given limitations of ionic liquid, gel or ferroelectric gating, experimental validations of gate-induced percolation may thus rely in most cases on chemically doping close to the percolation threshold. (ii) Once percolation is reached, the saturation magnetization M_s is largely enhanced due to the presence of critical clusters extending deep into the bulk. (iii) The existence of

ferromagnetic bulk clusters will also be reflected in the dependence of the magnetization $M_s(z)$ on the distance z from the surface. Our work thus shows that "bulk" magnetic properties can be controlled using "surface" electrostatic gating. In our approach, the transition to long-range ferromagnetic order in LSCO is driven solely by percolation, and not by order parameter fluctuations. While at low enough temperatures thermal fluctuations are indeed weak, quantum fluctuations remain present. However, previous studies of diluted quantum magnetic systems found that the percolation threshold and certain percolation critical exponents (such as β and ν) are unaffected by quantum fluctuations [35,36], even in the presence of dissipation [37,38], which is expected to occur on the metallic side of the transition. Finally, while we have focused on electrostatic gating, our conclusions also apply to electrochemical doping describing, for example, the transfer of oxygen vacancies into the surface of a sample.

We gratefully acknowledge useful discussions with K. Reich. This work was supported primarily by the National Science Foundation through the University of Minnesota MRSEC under Award No. DMR-1420013. We acknowledge the Minnesota Supercomputing Institute (MSI) at the University of Minnesota for providing resources that contributed to the research results of this work.

[1] P. Zubko, S. Gariglio, M. Gabay, P. Ghosez, and J.-M. Triscone, Annu. Rev. Condens. Matter Phys. **2**, 141 (2011).
[2] J. Ngai, F. Walker, and C. Ahn, Annu. Rev. Mater. Res. **44**, 1 (2014).
[3] J. A. Sulpizio, S. Ilani, P. Irvin, and J. Levy, Annu. Rev. Mater. Res. **44**, 117 (2014).
[4] J. H. Haeni, P. Irvin, W. Chang, R. Uecker, P. Reiche, Y. L. Li, S. Choudhury, W. Tian, M. E. Hawley, B. Craigo, A. K. Tagantsev, X. Q. Pan, S. K. Streiffer, L. Q. Chen, S. W. Kirchoefer, J. Levy, and D. G. Schlom, Nature (London) **430**, 758 (2004).
[5] A. Ohtomo and H. Hwang, Nature (London) **427**, 423 (2004).
[6] S. Stemmer and S. J. Allen, Annu. Rev. Mater. Res. **44**, 151 (2014).
[7] A. Bhattacharya and S. J. May, Annu. Rev. Mater. Res. **44**, 65 (2014).
[8] C. H. Ahn, A. Bhattacharya, M. Di Ventra, J. N. Eckstein, C. D. Frisbie, M. E. Gershenson, A. M. Goldman, I. H. Inoue, J. Mannhart, A. J. Millis, A. F. Morpurgo, D. Natelson, and J.-M. Triscone, Rev. Mod. Phys. **78**, 1185 (2006).
[9] C. H. Ahn, J.-M. Triscone, and J. Mannhart, Nature (London) **424**, 1015 (2003).
[10] A. M. Goldman, Annu. Rev. Mater. Res. **44**, 45 (2014).
[11] S. Asanuma, P.-H. Xiang, H. Yamada, H. Sato, I. H. Inoue, H. Akoh, A. Sawa, K. Ueno, H. Shimotani, H. Yuan, M. Kawasaki, and Y. Iwasa, Appl. Phys. Lett. **97**, 142110 (2010).
[12] R. Scherwitzl, P. Zubko, I. G. Lezama, S. Ono, A. F. Morpurgo, G. Catalan, and J.-M. Triscone, Adv. Mater. **22**, 5517 (2010).
[13] M. Nakano, K. Shibuya, D. Okuyama, T. Hatano, S. Ono, M. Kawasaki, Y. Iwasa, and Y. Tokura, Nature (London) **487**, 459 (2012).
[14] J. Jeong, N. Aetukuri, T. Graf, T. D. Schladt, M. G. Samant, and S. S. P. Parkin, Science **339**, 1402 (2013).
[15] K. Ueno, S. Nakamura, H. Shimotani, A. Ohtomo, N. Kimura, T. Nojima, H. Aoki, Y. Iwasa, and M. Kawasaki, Nat. Mater. **7**, 855 (2008).
[16] A. T. Bollinger, G. Dubuis, J. Yoon, D. Pavuna, J. Misewich, and I. Bozovic, Nature (London) **472**, 458 (2011).
[17] X. Leng, J. Garcia-Barriocanal, S. Bose, Y. Lee, and A. M. Goldman, Phys. Rev. Lett. **107**, 027001 (2011).
[18] H. J. A. Molegraaf, J. Hoffman, C. A. F. Vaz, S. Gariglio, D. van der Marel, C. H. Ahn, and J.-M. Triscone, Adv. Mater. **21**, 3470 (2009).
[19] Y. Yamada, K. Ueno, T. Fukumura, H. T. Yuan, H. Shimotani, Y. Iwasa, L. Gu, S. Tsukimoto, Y. Ikuhara, and M. Kawasaki, Science **332**, 1065 (2011).
[20] E. Dagotto, T. Hotta, and A. Moreo, Phys. Rep. **344**, 1 (2001).
[21] A. N. Pasupathy, A. Pushp, K. K. Gomes, C. V. Parker, J. Wen, Z. Xu, G. Gu, S. Ono, Y. Ando, and A. Yazdani, Science **320**, 196 (2008).
[22] J. Wu and C. Leighton, Phys. Rev. B **67**, 174408 (2003).
[23] C. He, S. El-Khatib, J. Wu, J. W. Lynn, H. Zheng, J. F. Mitchell, and C. Leighton, Europhys. Lett. **87**, 27006 (2009).
[24] B. I. Shklovskii and A. L. Efros, *Electronic Properties of Doped Semiconductors*, Springer Series in Solid-State Sciences Vol. 45 (Springer, Heidelberg, 1984).
[25] D. Stauffer and A. Aharony, *Introduction to Percolation Theory*, 2nd ed. (Taylor & Francis, London, 1994).
[26] C. He, S. El-Khatib, S. Eisenberg, M. Manno, J. W. Lynn, H. Zheng, J. F. Mitchell, and C. Leighton, Appl. Phys. Lett. **95**, 222511 (2009).
[27] T. Vojta and J. Schmalian, Phys. Rev. Lett. **95**, 237206 (2005).
[28] R. Yu, T. Roscilde, and S. Haas, Phys. Rev. Lett. **94**, 197204 (2005).
[29] N. Bray-Ali, J. E. Moore, T. Senthil, and A. Vishwanath, Phys. Rev. B **73**, 064417 (2006).
[30] L. Wang and A. W. Sandvik, Phys. Rev. Lett. **97**, 117204 (2006).
[31] R. M. Fernandes and J. Schmalian, Phys. Rev. Lett. **106**, 067004 (2011).
[32] J. Wang, Z. Zhou, W. Zhang, T. M. Garoni, and Y. Deng, Phys. Rev. E **87**, 052107 (2013).
[33] M. E. J. Newman and R. M. Ziff, Phys. Rev. Lett. **85**, 4104 (2000).
[34] M. E. J. Newman and R. M. Ziff, Phys. Rev. E **64**, 016706 (2001).
[35] T. Senthil and S. Sachdev, Phys. Rev. Lett. **77**, 5292 (1996).
[36] A. W. Sandvik, Phys. Rev. B **66**, 024418 (2002).
[37] M. Al-Ali, J. A. Hoyos, and T. Vojta, Phys. Rev. B **86**, 075119 (2012).
[38] J. A. Hoyos and T. Vojta, Phys. Rev. B **74**, 140401 (2006).